Published in final edited form as:
Gastroenterology. 2011 April ; 140(4): 1303–1313.e3. doi:10.1053/j.gastro.2010.12.039.

Inactivation of Brca2 promotes Trp53-associated but inhibits KrasG12D-dependent pancreatic cancer development in mice

Matthew Rowley[1], **Akihiro Ohashi**[1], **Gourish Mondal**[1], **Lisa Mills**[1], **Lin Yang**[1], **Lizhi Zhang**[1], **Rhianna Sundsbak**[2], **Virginia Shapiro**[2], **Michael Muders**[3], **Thomas Smyrk**[1], and **Fergus J. Couch**[1]

[1] Department of Laboratory Medicine and Pathology, Mayo Clinic, Rochester, Minnesota, 55905

[2] Department of Immunology, Mayo Clinic, Rochester, Minnesota, 55905

[3] Department of Urology, Mayo Clinic, Rochester, Minnesota, 55905

Abstract

Background & Aims—Inherited mutations in the *BRCA2* tumor suppressor have been associated with an increased risk of pancreatic cancer. To establish the contribution of *Brca2* to pancreatic cancer we developed a mouse model of pancreas-specific *Brca2* inactivation. Since BRCA2 inactivating mutations cause defects in repair of DNA double-strand breaks that result in chromosomal instability, we evaluated whether *Brca2* inactivation induced instability in pancreatic tissue from these mice and whether associated pancreatic tumors were hypersensitive to DNA damaging agents.

Methods—We developed mouse models that combined pancreas-specific *Kras* activation and *Trp53* deletion with *Brca2* inactivation. Development of pancreatic cancer was assessed; tumors and non-malignant tissues were analyzed for chromosomal instability and apoptosis. Cancer cell lines were evaluated for sensitivity to DNA damaging agents.

Results—In the presence of disrupted *Trp53, Brca2* inactivation promoted development of premalignant lesions and pancreatic tumors that reflected the histology of the human disease. Cancer cell lines derived from these tumors were hypersensitive to specific DNA damaging agents. In contrast, in the presence of *KrasG12D, Brca2* inactivation promoted chromosomal instability and apoptosis and unexpectedly inhibited growth of premalignant lesions and tumors.

Conclusions—*Trp53* signaling must be modified before inactivation of the *Brca2* wild-type allele, irrespective of *Kras* status, for *Brca2*-deficient cells to form tumors.

Keywords

pancreas; cancer genetics; oncogene; neoplasia

Address Correspondence to: Dr. F.J. Couch, Department of Laboratory Medicine and Pathology, Mayo Clinic, 200 First Street SW, Rochester, MN 55905. Tel: 507 284-3623 Fax: 507 538-1937 couch.fergus@mayo.edu.

Author contributions:
MR: acquisition of data, analysis and interpretation of data, statistical analysis, drafting of the manuscript
AO, GM, LM, LY, LZ, RS, MM, TS, VS: acquisition of data; critical revision of the manuscript for important intellectual content
FJC: study concept and design, analysis and interpretation of data, critical revision of the manuscript

Disclosures: The authors have no conflicts to disclose.

Introduction

The *BRCA2* gene encodes a 3418 amino acid protein that is a key component of the homology-directed DNA repair pathway[1,2] and is involved in maintenance of structural and numerical chromosomal stability. While germline mutations in BRCA2 predispose to breast and ovarian cancer[3], an increased risk (relative risk, 5.54) of pancreatic ductal adenocarcinoma (PDAC) was also observed among BRCA2 mutation carriers from 173 breast and ovarian cancer families[3]. In addition, germline mutations in BRCA2 are among the most common genetic lesions associated with familial pancreatic cancer[4,5] and somatic BRCA2 mutations have been associated with 10% of sporadic pancreatic cancers[6,7]. Mutations in PALB2 and the FANCC and FANCG Fanconi anemia complex components that interact with BRCA2 have also been implicated in pancreatic cancer[8]. While these studies suggest a role for BRCA2 in pancreatic cancer, direct evidence of the contribution of BRCA2 to pancreatic cancer development remains to be elucidated.

Histological analysis of PDAC has identified a common pattern of disease progression from pancreatic intraepithelial neoplasia (PanIN) precursor lesions with increasingly severe stages of cellular atypia to invasive tumors[9]. Common genetic lesions associated with the development and progression of this disease have been identified including KRAS activating mutations in >90% of PDAC cases[10] that occur early in tumor development and TP53 mutations in 50–70% of tumors[11] that occur late in tumor development[12], similarly to BRCA2 mutations[9]. Conditional activation of Kras alone and in combination with inactivation of tumor suppressors such as *Trp53* in the pancreas of mouse models has been shown to promote formation of PanINs and invasive tumors[13]. Here we utilized these models in combination with a conditional knockout mouse model of Brca2 to demonstrate a direct role for BRCA2 in pancreatic cancer.

Results

To evaluate the role of BRCA2 in pancreatic cancer we used a mouse model expressing a functional wild type *Brca2* gene, in which exon 11 of *Brca2* is flanked by *lox*P sites ($B2^{F11}$)[14]. Conditional rearrangement of this allele in the developing pancreas in response to *pdx-1-cre*(C) expression resulted in deletion of *Brca2* exon 11, and the generation of a functionally null *brca2* allele ($B2^{\Delta 11}$)[14] (Figure 1A). *TP53* is frequently mutated in *BRCA2* associated breast and ovarian tumors[15], and mutations in *Brca2* and *Trp53* act synergistically to promote tumorigenesis in mouse mammary glands[14]. Therefore, we crossed $CB2^{\Delta 11/\Delta 11}$ mice with conditional $Trp53^{F2\text{-}10/F2\text{-}10}$ (P) mice, in which exons 2 and 10 were flanked by *lox*P sites[14] (Figure 1A), to ultimately generate *Trp53*-null $CPB2^{\Delta 11/\Delta 11}$, $CPB2^{wt/\Delta 11}$ *and* $CPB2^{wt/wt}$ mice. Allele-specific PCR of DNA extracted from tail snip and pancreas DNA demonstrated that the floxed alleles of *Brca2* and *Trp53* were present in the tail and that these alleles were efficiently rearranged by Cre recombinase in the pancreas (Figure 1B).

$CPB2^{\Delta 11/\Delta 11}$(n=47), $CPB2^{wt/\Delta 11}$(n=41), and $CPB2^{wt/wt}$ (n=34) mice were aged and evaluated for pancreatic tumor development. $CPB2^{\Delta 11/\Delta 11}$ mice developed pancreatic cancer at high frequency (median survival of 300 days) and exhibited substantially reduced pancreatic cancer-free survival relative to $CPB2^{wt/\Delta 11}$ mice ($p<0.0001$) and $CPB2^{wt/wt}$ mice ($p<0.0001$) (Figure 1C). In contrast, $CB2^{\Delta 11/\Delta 11}$(n=12), $CB2^{wt/\Delta 11}$(n=21), and $CB2^{wt/wt}$ (n=18) mice expressing wildtype *Trp53* alleles failed to develop PDAC. Efficient rearrangement of alleles in these mice was verified by PCR. Histological evaluation of serial sections from all pancreas glands from the $CB2^{\Delta 11/\Delta 11}$, $CB2^{wt/\Delta 11}$ and $CB2^{wt/wt}$ mice at 24 months of age confirmed the absence of precursor lesions or PDAC. In addition, immunohistochemistry (IHC) with antibodies against cytokeratin 19 (CK19), amylase and

insulin identified normal ductal, acinar, and islet cell components of the pancreas (Figure S1A). These findings suggest that inactivation of Brca2 alone does not promote pancreatic cancer development, but that disruption of Trp53 signaling in combination with inactivation of Brca2 significantly enhances pancreatic tumor formation. In addition, the results show that disruption of Trp53, by deletion of exons 2–10, can promote pancreatic cancer with long latency.

The pancreatic tumors observed in the CPB2$^{\Delta 11/\Delta 11}$ mice were histologically similar to human pancreatic cancers. Over 40% resembled human tubular PDAC (Figure 1D) and stained positive for CK19 and negative for amylase by IHC (Figure 1E, panel ii–iii), suggesting a ductal origin. Another 15% of tumors were acinar carcinomas that stained positive for amylase and negative for CK19 (Figure 1E, panel xi–xii). A further 35% were high grade undifferentiated carcinomas. Since 50% were negative for CK19 and amylase (Figure 1E, panels v–vi) and 50% were negative for CK19 but positive for amylase (Figure 1E, panels viii–ix), the cell of origin of these tumors is uncertain. The final 20% were mucinous tumors. There was no evidence of significant desmoplastic stroma in any of these tumors. The proportion of tumors from CPB2$^{wt/\Delta 11}$ mice in each histological subgroup was remarkably consistent with those from CPB2$^{\Delta 11/\Delta 11}$ mice. However, tumors forming in CPB2$^{wt/wt}$ mice were predominantly acinar and undifferentiated. Since both the B2^{wt} and B2$^{\Delta 11}$ alleles were expressed in cell lines derived from tumors in CPB2$^{wt/\Delta 11}$ mice (data not shown), it appears that the similarity in histology of tumors from CPB2$^{wt/\Delta 11}$ and CPB2$^{\Delta 11/\Delta 11}$ mice was not the result of somatic loss of the wildtype allele in the pancreas tissue from CPB2$^{wt/\Delta 11}$ mice. Alternatively, since *Brca2* may exhibit haploinsufficiency in murine pancreatic tissue[16], it is possible that the inactivation of a single allele of *Brca2* may influence the tumor histology but not tumor frequency in these mice.

Next we evaluated pancreas glands from 8 month-old mice without invasive pancreatic cancer for the presence of premalignant lesions. CPB2$^{\Delta 11/\Delta 11}$ mice displayed severe acinar cell dysplasia and reduced numbers of islets (72%) (Figure 1F, panel i–ii). The pancreata were severely atrophic (60%) with acini replaced by mature adipose tissue. Mild focal acute and chronic inflammatory infiltrate (67%) with little evidence of fibrosis was also evident. In contrast, dysplasia (<8%), atrophy (<9%), and chronic inflammatory infiltrate (<14%) was less severe and less frequent in age matched CPB2$^{wt/\Delta 11}$ and CPB2$^{wt/wt}$ mice. Similar evaluation of pancreatic tissue from CPB2$^{\Delta 11/\Delta 11}$ mice harvested during resection of tumors or at time of death identified PanIN lesions in 66% and flat epithelial high grade dysplasia in 72% of the pancreas glands. In contrast, PanINs were observed in <6% of pancreas glands from the aged CPB2$^{wt/\Delta 11}$ and CPB2$^{wt/wt}$ mice. Thus, combined disruption of *Brca2* and *Trp53*, but not disruption of *Brca2* or *Trp53* alone, causes extensive remodeling of the pancreas and rapid development of premalignant and malignant lesions.

To confirm that the CPB2$^{\Delta 11/\Delta 11}$ tumors displayed a BRCA2 null phenotype we characterized a series of early passage tumor cell lines (Figure S2A) from CPB2$^{\Delta 11/\Delta 11}$, CPB2$^{wt/\Delta 11}$, and CPB2$^{wt/wt}$ mice. Cells with defects in BRCA2 and other HR DNA repair pathway proteins display chromosomal aberrations and defective Rad51 focus formation in response to DNA damage[1]. Here we showed that cells from CPB2$^{\Delta 11/\Delta 11}$ tumors displayed increased inter-chromosomal radial structures relative to CPB2$^{wt/\Delta 11}$ and CPB2$^{wt/wt}$ cells, in response to mitomycin-c (MMC) treatment (Figure 2D and S2B). Similarly, CPB2$^{\Delta 11/\Delta 11}$ cells exhibited decreased Rad51 foci, but not γH2AX foci (Figure S2C). Recently, it has been shown that cells deficient in BRCA2 are hypersensitive to poly-ADP-ribose polymerase (PARP) inhibitors[17,18] and DNA cross-linking agents such as cisplatin[19]. Consistent with these observations, we found that CPB2$^{\Delta 11/\Delta 11}$ tumor cell lines displayed increased sensitivity to the PARP inhibitor ABT-888 and to cisplatin, but not to gemcitabine

(Figure 2A–C). These results suggest that these and agents that promote replication defects may be useful in treating pancreatic tumors with BRCA2 mutations.

BRCA2 deficient tumors display numerical as well as structural chromosomal instability. Aneuploid cells may derive from impaired DNA damage repair and/or aberrant chromosomal segregation, whereas polyploidy cells may result from failure of cytokinesis[20,21]. Here immunofluorescence microscopy showed that CPB2$^{\Delta 11/\Delta 11}$ tumor cell lines exhibited elevated levels of multinucleation and centrosome amplification (Figure 2E). Similarly, metaphase spreads verified increased aneuploidy and polyploidy in these cells (Figure 2F). Furthermore, multinucleated cells were frequently detected in H&E stained sections of CPB2$^{\Delta 11/\Delta 11}$ tumors (Figure 1F, panel iii). Because of the significantly elevated levels of polyploidy in CPB2$^{\Delta 11/\Delta 11}$ cells we investigated the influence of Brca2 on cytokinesis. We verified the absence of Brca2, but not CEP55, from the midbody in *brca2*$^{\Delta 11/\Delta 11}$ cells by immunofluorescence staining. Similarly, endosomal membrane resorting complex (ESCRT) proteins, such as CHMP1B, that are involved in the final stage of cytokinesis, were reduced or absent from the midbodies of BRCA2 null cells (CPB2$^{\Delta 11/\Delta 11}$ and PEO1 cells), relative to their wildtype counterparts (CPB2$^{wt/wt}$ and PEO4) (Figure 3A). Reconstitution of CPB2$^{\Delta 11/\Delta 11}$ cells with GFP-tagged wildtype BRCA2 (Figure 3B and 3C), enhanced recruitment of membrane-associated endobrevin to the midbody and substantially reduced the levels of multinucleation and centrosome amplification over a 72 hr period (Figure 3D), suggesting a direct role for BRCA2 in regulation of numerical chromosomal instability.

Since Brca2 deficiency in combination with inactivation of Trp53 promoted pancreatic cancer in mice, we further evaluated whether disruption of Brca2 also enhanced pancreatic tumor formation in a *pdx-1-cre* dependent activated *Kras*^{G12D} (CK) mouse model[13] (Figure 4A). Allele-specific PCR verified the presence of floxed *Brca2*^{F11} and *LSL-Kras*^{G12D} alleles in the tail and cre recombinase-dependent rearranged alleles in the pancreas (Figure 4B). CKB2$^{\Delta 11/\Delta 11}$, CKB2$^{wt/\Delta 11}$ and CKB2$^{wt/wt}$ mice displayed normal pancreatic development and normal ductal, acinar, and islet cell architecture (Figure 4C, panels i–iv), although 20% of CKB2$^{\Delta 11/\Delta 11}$ mice exhibited pancreatic insufficiency due to replacement of acinar tissue with adipose tissue at young age. Histological evaluation of serial sections from pancreas glands of 8 month old CKB2$^{wt/\Delta 11}$ and CKB2$^{wt/wt}$ mice detected PanINs (Figure 4C, panel viii and xii) and metaplastic lesions (Figure 4C, panels v–vii), with an average of 4.3 and 3.7 PanIN lesions per section (Figure 4D) and an average of 10.2 and 11.1 transdifferentiation/metaplastic lesions per section[22] (Figure 4E). In contrast, only 0.14 PanIN lesions and 0.24 metaplastic lesions per section were observed in CKB2$^{\Delta 11/\Delta 11}$ mice (Figure 4D and 4E). Consistent with these findings, only 13% (4/30) of CKB2$^{\Delta 11/\Delta 11}$ mice developed tumors (Figure 4F), whereas 66% (23/35) of CKB2$^{wt/\Delta 11}$ ($p=0.0095$) and 61% (17/28) of CKB2$^{wt/wt}$ ($p=0.0028$) mice developed pancreatic tumors with an average latency of 366 and 406 days, respectively. The rate of tumor development did not differ between CKB2$^{wt/\Delta 11}$ and CKB2$^{wt/wt}$ mice ($p=0.696$). The majority of the tumors (90%) in CKB2$^{wt/\Delta 11}$ and CKB2$^{wt/wt}$ mice, and the four tumors arising in CKB2$^{\Delta 11/\Delta 11}$ mice, were CK19-positive and amylase-negative pancreatic ductal adenocarcinomas (Figure 4C, panels ix–xi). Thus, loss of the *Brca2* tumor suppressor gene inhibits the development of premalignant lesions and pancreatic tumors that are induced by activated *Kras*.

Since inactivated *Brca2* inhibited *Kras*^{G12D} associated pancreatic cancer but acted synergistically with disrupted *Trp53* to promote pancreatic cancer, we evaluated whether Kras activation and Trp53 disruption co-occurred in tumors derived from these animal models. The four tumors from CKB2$^{\Delta 11/\Delta 11}$ mice stained strongly positive for Trp53 expression suggesting the presence of *Trp53* mutations. In addition, we successfully PCR amplified and sequenced all *Trp53* exons from DNA extracted from one paraffin-embedded

tumor and identified an alteration encoding a C239R missense mutation (Figure S3B) that was predicted by sequence conservation analysis (http://agvgd.iarc.fr) to disrupt Trp53 activity. Thus, $Kras^{G12D}$ tumors arising in the absence of Brca2 appeared to require inactivation of Trp53 signaling pathways. In contrast, sequencing of the *Kras* gene in six ductal, five undifferentiated, and two acinar tumors from $CPB2^{\Delta 11/\Delta 11}$ mice yielded activating Kras mutations (G12D) in only one ductal and one undifferentiated tumor (Figure S3A), indicating that Kras activation was rarely associated with Brca2 associated pancreatic cancer.

Next we evaluated biomarkers for signaling pathways commonly altered in pancreatic cancers in the tumors from the $CPB2^{wt/wt}$, $CPB2^{\Delta 11/\Delta 11}$, $CKB2^{wt/wt}$, and $CKB2^{\Delta 11/\Delta 11}$ mice. The Notch ligand and the Notch target, Hes1, have been implicated in PanIN development through induction of transdifferentiation of acinar cells to ductal-like cells[13]. Additionally, Sonic hedgehog (Shh) is upregulated in early PanIN lesions, and is often associated with Kras mutations in PDAC[23]. Hes1 expression levels in the tumors did not differ (Figure 5, panels i–iii), whereas Shh levels were higher in CKB2 tumors than in CPB2 tumors (Figure 5, panels iv–vi). The status of the *brca2* gene appeared to have no effect on either Hes1 or Shh expression levels. β-catenin has been shown to inhibit Kras dependent transdifferentiation of acinar cells into PanIN lesions[24]. Here β-catenin expression was elevated but did not differ among the various tumors. In contrast, the neuroendocrine marker synaptophysin displayed low expression, suggesting that the tumors did not originate among islet cells (data not shown). Proliferation measured by Ki-67 staining was markedly increased in CPB2 tumors compared to CKB2 tumors, presumably due to the loss of p53 dependent cell cycle control (Figure 5, panels vii–ix). Also, CKB2 but not CPB2 tumors displayed high levels of phospho-Erk1/2, consistent with the effects of activated Kras (Figure 5, panels x–xii). Finally, alcian blue staining confirmed that the tumors and PanIN lesions in CKB2 mice but not CPB2 mice were highly mucinous (Figure 5, panels xiii–xv). These results suggest that tumors involving disruption of the *Trp53* gene follow different developmental pathway from tumors associated with Kras activation.

Given the role of BRCA2 in regulation of chromosomal instability and the increased numerical chromosomal instability in $CPB2^{\Delta 11/\Delta 11}$ mice, we evaluated the influence of Brca2 on instability in the presence of $Kras^{G12D}$. Fluorescent in situ hybridization (FISH) studies of pancreas tissue from 8 month old mice using murine chromosome 9 and 12 centromeric probes detected elevated chromosome copy number in pancreas glands of $CKB2^{\Delta 11/\Delta 11}$ mice relative to $CKB2^{wt/wt}$ mice (Figure 6A and S4A). This suggests that inactivation of Brca2 significantly enhanced levels of numerical chromosomal instability *in vivo*. Similarly, mouse embryonic fibroblasts (MEFs) from $CKB2^{\Delta 11/\Delta 11}$ mice, infected with adenoviral-cre to rearrange the *Brca2* and *Kras* loci (Figure S4B), displayed elevated levels of aneuploidy and multinucleation relative to MEFs from $CKB2^{wt/wt}$ mice, in both the presence and absence of $Kras^{G12D}$ (Figure 6B and 6C). To evaluate whether the structural and numerical chromosomal instability resulting from *Brca2* deficiency resulted in elevated levels of cell death in the presence of *Trp53* disruption and activated Kras, we measured *in vivo* apoptosis by cleaved caspase 3 staining of acinar and ductal cells in the pancreas glands of 4 month old mice. Levels of apoptosis were increased 2-fold in $CPB2^{\Delta 11/\Delta 11}$ mice relative to $CPB2^{wt/wt}$ mice (Figure 6D), suggesting that the instability caused by absence of Brca2 enhances apoptosis. However, the levels of apoptosis were equivalent in $CPB2^{\Delta 11/\Delta 11}$ and $CB2^{\Delta 11/\Delta 11}$ pancreata. Thus, apoptosis resulting from *Brca2* deficiency *in vivo* may not be dependent on *Trp53* status. In contrast, 4 month old $CKB2^{\Delta 11/\Delta 11}$ mice displayed 8.6-fold higher levels of *in vivo* apoptosis than $CKB2^{wt/\Delta 11}$ and $CKB2^{wt/wt}$ mice (Figure 6E and S4C), suggesting that activated Kras and inactive Brca2 co-operate to promote cell death.

Discussion

Germline mutations in the *BRCA2* gene have been observed in pancreatic cancer families and *BRCA2* mutations have been detected in unselected adenocarcinomas from the pancreas, suggesting a role for BRCA2 in the development of pancreatic cancer. Here we show, using a pancreas specific knockout mouse model, that disruption of *Brca2* promotes the development and progression of pancreatic cancer when combined with *Trp53* inactivation, but not in the presence of active Trp53 signaling. Based on our findings we suggest a model, whereby disruption of Trp53 signaling occurs prior to inactivation of the second *Brca2* allele. In this model, inactive Trp53 signaling allows pancreatic cells to evade the growth inhibitory or cell death[14] effects caused by the extensive numerical and structural instability that develops in the absence of functional Brca2 protein (Figure 7). This is consistent with the presence of *TP53* mutations in human PDACs containing *BRCA2* mutations[25]. The model further suggests that loss of the wildtype *BRCA2* allele in human carriers of germline *BRCA2* mutations must occur late in the pancreatic tumor development process after the inactivation of TP53 signaling. Support for this comes from studies of human PDAC, which showed that the loss of heterozygosity (LOH) of *BRCA2* appears to be a late event in tumorigenesis[9,26].

Somewhat surprisingly our studies also showed that inactivation of *Brca2* inhibits development of PanINs, metaplastic lesions and PDAC in the well-characterized *pdx-1-cre;LSL-Kras*^{G12D} mouse model. This synthetic lethal effect appears to be associated with the increased chromosomal instability caused by Brca2 deficiency with some evidence suggesting a synergistic effect of Kras activation and Brca2 disruption on apoptosis (Figure 6E). Given our data suggesting that the few pancreatic tumors arising in CKB2$^{\Delta 11/\Delta 11}$ mice contained *Trp53* mutations, and the known presence of *BRCA2*, *TP53* and *Kras*^{G12V} mutations in the human Capan-1 pancreatic cancer cell line, the suggestion is that disruption of Trp53 signaling is again required to bypass the effects of Brca2 inactivation in cells expressing Kras^{G12D}. While we were unable to generate sufficient numbers of CKPB2$^{\Delta 11/\Delta 11}$ mice to confirm this model, a pancreas specific CKPB2$^{Tr/\Delta 11}$ model involving a Trp53^{R270H} allele instead of a Trp53 truncating mutation and a Brca2^{Tr} allele that truncates Brca2 at amino acid 1492 has recently been described[16]. These CKPB2$^{Tr/\Delta 11}$ mice develop pancreatic tumors at high frequency, which in part supports the model that Trp53 disruption is required for tumor formation in Brca2 deficient pancreata, both in the presence and absence of activated Kras. However, in the same report it was suggested that CKB2$^{Tr/\Delta 11}$ mice developed pancreatic cancer in the presence of wildtype Trp53, an observation that would appear to be contrary to our proposed model. Careful examination of the presented PDAC-free Kaplan-Meier survival estimates suggests that only a small number/proportion of CKB2$^{Tr/\Delta 11}$ mice developed pancreatic tumors[16], fully consistent with the 13% tumor incidence at 500 days in our CKB2$^{\Delta 11/\Delta 11}$ mice (Figure 4F). Should the tumors arising in the CKB2$^{Tr/\Delta 11}$ mice contain Trp53 mutations or exhibit altered Trp53 signaling, similarly to the four tumors from our CKB2$^{\Delta 11/\Delta 11}$ mice, then the results would further support the proposed model. Since the Trp53 status of the tumors was not reported, additional studies of pancreatic tumors arising in these mice are needed. Furthermore, whether aberrations in other regulators of apoptosis and cell cycle can rescue the effects of *Brca2* deficiency remains to be determined. Taken together, our results point to critical temporal regulation of the second *BRCA2* “hit” and the importance of the interplay between *BRCA2* and *TP53* for development of PDAC.

The variety of different tumor types observed in the CPB2$^{\Delta 11/\Delta 11}$ mice suggests a high degree of plasticity among cells of the pancreas. We noted that CPB2$^{wt/wt}$ mice displayed predominantly acinar tumors, whereas additional inactivation of Brca2 in CPB2$^{\Delta 11/\Delta 11}$ mice reduced the frequency of acinar tumors and promoted formation of ductal-like tumors.

Similarly, disruption of other tumor suppressor genes in the pancreas has promoted development of other types of pancreatic tumors. In particular, *pdx-1-cre;Ink4a*$^{-/-}$*;LSL-Kras*^{G12D} mice develop tumors of spindle cell or sarcomatoid histology[27], while *pdx-1-cre;Smad4*$^{-/-}$*;LSL-Kras*^{G12D} mice develop intraductal papillary mucinous neoplasia (IPMN)[28]. Furthermore, it is now well established that Kras^{G12D} expression promotes transdifferentiation of acinar cells to ductal-like cells in *pdx-1-cre;LSL-Kras*^{G12D} mice. Thus, the temporality of these alterations in combination with the roles of specific signaling pathways in development and differentiation may influence the histology of the resulting tumors. Alternatively, pancreatic tumors of different tumor histology may arise from effects on progenitor cells in the murine pancreas[29,30]. Studies have shown that expression of PyMT in the murine pancreas induces tumors with different histological features that express the pancreatic progenitor marker pdx-1 and/or markers of other cell lineages, suggesting that a progenitor cell that can differentiate into cells of different lineages may be the tumor cell of origin[29].

The role of BRCA2 in homology directed repair of DNA double strand breaks is well-established. However, a role for BRCA2 in regulation of cytokinesis and cell division has also been proposed, based on frequent multinucleation in *Brca2*$^{-/-}$ ES cells, localization of BRCA2 to intercellular bridges and abnormalities in myosin II organization at the cleavage furrow following depletion of BRCA2[20]. Here we show that up to 30% of cells from CPB2$^{\Delta 11/\Delta 11}$ tumor cell lines display multinucleation and polyploidy, whereas only 5% of CPB2$^{wt/wt}$ tumor cells show similar effects (Figure 2E and 2F). Similarly B2$^{\Delta 11/\Delta 11}$ MEFs display increases in unresolved cytokinetic bridge structures and multinucleation relative to B2$^{wt/wt}$ MEFs. In addition, the localization of Brca2 to the midbody and the reduced levels of membrane remodeling complexes at the midbody in response to Brca2 inactivation suggest that disruption of Brca2 may result in delays in or failure of cytokinesis because of inefficient membrane remodeling at the midbody. Our findings suggest that disruption of BRCA2 activity at the midbody may contribute to the numerical instability observed in all BRCA2 deficient cells and may contribute to tumorigenesis.

The studies reported here may have significant therapeutic implications. Specifically, we have verified that Brca2 deficient pancreatic tumors display enhanced sensitivity to cisplatin and PARP inhibitors but not DNA damaging agents such as Gemcitabine. These effects are consistent with the response to PARP inhibitors observed in a CKPB2$^{Tr/\Delta 11}$ murine model of Brca2 deficient pancreatic cancer[16] and in breast, ovarian and prostate cancer patients with germline BRCA2 mutations[31]. Recent phase 2 clinical trials also suggest that PARP inhibitors can be used successfully to treat cancer patients with germline mutations in BRCA1 or BRCA2[32]. Our findings suggest that human pancreatic tumors arising in individuals with germline BRCA2 mutations may be particularly sensitive to PARP inhibitors and other agents that induce similar replication defects. The mouse model of *Brca2*-associated inherited pancreatic cancer described here may also prove useful for further characterization of the *in vivo* response to these therapeutics.

Experimental Procedures

Transgenic mice

Conditional *Brca2*^{F11}, *LSL-Kras*$^{G12D/+}$, *Trp53*$^{F2\text{-}10}$, and *pdx-1-cre* mice were as previously described[13,14]. Mice were housed in a specific pathogen free facility and were interbred to generate the cohorts of mice used in this study. All experiments were conducted in compliance with Mayo Clinic IACUC guidelines.

Genotyping

DNA was harvested from mouse tails using the DNeasy Blood and Tissue Kit (Qiagen) and genotyped by PCR. Reaction conditions for *Brca2*, *Trp53*, and *Cre* were 36 cycles of 94°C for 30 sec, 56°C for 30 sec, and 72°C for 1 min. Conditions for *Kras* were 40 cycles of 94°C for 30 sec, 63°C for 30 sec and 72°C for 1 min. Genotyping primers are listed in supplemental information.

Histology and immunohistochemistry

Pancreatic tissue from mice was fixed in 10% formalin overnight and embedded in paraffin. Slides were deparaffinized in xylene and rehydrated. Antigen retrieval was carried out in citrate buffer. Slides were incubated with H_2O_2 and blocked in Rodent Block Mouse (Biocare Medical, Walnut Creek, CA) for 20 minutes. Sections were incubated in primary antibody for 60 minutes and incubated with HRP conjugated secondary antibody. Slides were further incubated in diaminobenzidine (DAB+) (DAKO) and counterstained with Modified Schmidts' Hematoxylin.

Chromosome enumeration of metaphase spreads

$1–2\times10^6$ cells were treated with 0.05 μg/ml colcemid (GIBCO BRL) for 5–6 h at 37°C. Cells were harvested, suspended in KCl and fixed in Carnoy's solution (75% methanol, 25% acetic acid). 10–20 μl aliquots were dropped onto glass slides, stained in 5% Giemsa solution, and analyzed on an Olympus AX70 microscope using a 100× objective. For MMC response, cells were treated with 100nM MMC for 1 hour and 48 hours later were harvested for metaphase spreads.

Immunofluorescence

Cells grown on glass slides were fixed with 3% paraformaldehyde and permeabilized with 0.2% TritonX-100. Slides were blocked in 3% non-fat milk and incubated with primary antibodies overnight. Slides were then incubated with secondary antibodies for 2–3 hours, fixed with 3% paraformaldehyde and mounted with Prolong-anti-fade containing DAPI (Molecular Probes). Slides were imaged using a Zeiss LSM510 confocal microscope. Antibodies used are listed in supplemental information.

Tumor cell culture and transfection

Mouse pancreatic tumor tissue was minced and seeded in DMEM supplemented with 10% fetal bovine serum to establish tumor cell lines. Confluent cells were trypsinized and reseeded 1:3. Transfections were carried out using Lipofectamine Plus (Invitrogen).

Drug response

Mouse tumor cell lines were grown in 6-well plates in the presence of ABT-888, Gemcitabine, and cisplatin at the indicated dose for 6 days. Cells were harvested and resuspended in hypotonic propidium iodide solution (50 μg/mL propidium iodide) and analyzed by fluorescent activated cell sorting (FACS). Apoptotic cells were quantified as the percent of sub-diploid cells in the population.

Kras and *Trp53* mutation screens

Tumor tissue was macrodissected from 4 to 8 unstained 5μM paraffin sections and DNA was isolated using the QIAamp DNA mini kit (Qiagen). PCR fragments containing codons 12, 13, and 61 of Kras or all exons of *Trp53* were amplified with 40 cycles of 94°C for 30 sec, 56°C for 30 sec, 72°C for 1 min. PCR products were treated with ExosapIT and

subjected to bidirectional DNA sequencing in the Mayo Clinic DNA sequencing core using primers listed in supplemental information.

Isolation of MEFs

Pregnant female mice were euthanized at d12.5 and embryos were surgically removed from the abdomen. Embryos were minced, transferred to a 12 well culture plate, incubated at 37°C/5% $C0_2$ for 15 minutes, and re-homogenized for 3 cycles. Cells were collected, centrifuged at 1000rpm for 5 minutes and plated in DMEM. Experiments were performed on passage 3 to 6 cells.

FISH

Centrosomal DNA probe working solution was hybridized to 5μm paraffin sections previously deparaffinized in CitriSolv and treated with 10mM Citric Acid. DAPI counterstain was applied and visualization of FISH signals was accomplished using a fluorescent microscope.

Supplementary Material

Refer to Web version on PubMed Central for supplementary material.

Acknowledgments

Grant Support: This study was supported by an NCI Specialized Program of Research Excellence (SPORE) grant (CA102701) in pancreatic cancer at Mayo Clinic.

Abbreviations

B2	Brca2
C	Cre
K	Kras
P	Trp53, PanIN, pancreatic intraepithelial neoplasia
PDAC	pancreatic ductal adenocarcinoma

References

1. Moynahan ME, Pierce AJ, Jasin M. BRCA2 is required for homology-directed repair of chromosomal breaks. Mol Cell. 2001; 7:263–72. [PubMed: 11239455]
2. Tutt A, Bertwistle D, Valentine J, et al. in Brca2 stimulates error-prone homology-directed repair of DNA double-strand breaks occurring between repeated sequences. Embo J. 2001; 20:4704–16. [PubMed: 11532935]
3. Consortium TBCL. Cancer risks in BRCA2 mutation carriers. J Natl Cancer Inst. 1999; 91:1310–6. [PubMed: 10433620]
4. Couch FJ, Johnson MR, Rabe K, et al. Germ line Fanconi anemia complementation group C mutations and pancreatic cancer. Cancer Res. 2005; 65:383–6. [PubMed: 15695377]
5. Murphy KM, Brune KA, Griffin C, et al. Evaluation of candidate genes MAP2K4, MADH4, ACVR1B, and BRCA2 in familial pancreatic cancer: deleterious BRCA2 mutations in 17%. Cancer Res. 2002; 62:3789–93. [PubMed: 12097290]
6. Goggins M, Schutte M, Lu J, et al. Germline BRCA2 gene mutations in patients with apparently sporadic pancreatic carcinomas. Cancer Res. 1996; 56:5360–4. [PubMed: 8968085]
7. Ozcelik H, Schmocker B, Di Nicola N, et al. Germline BRCA2 6174delT mutations in Ashkenazi Jewish pancreatic cancer patients. Nat Genet. 1997; 16:17–8. [PubMed: 9140390]

8. Jones S, Hruban RH, Kamiyama M, et al. Exomic sequencing identifies PALB2 as a pancreatic cancer susceptibility gene. Science. 2009; 324:217. [PubMed: 19264984]
9. Hruban RH, Wilentz RE, Kern SE. Genetic progression in the pancreatic ducts. Am J Pathol. 2000; 156:1821–5. [PubMed: 10854204]
10. Almoguera C, Shibata D, Forrester K, et al. Most human carcinomas of the exocrine pancreas contain mutant c-K-ras genes. Cell. 1988; 53:549–54. [PubMed: 2453289]
11. Redston MS, Caldas C, Seymour AB, et al. p53 mutations in pancreatic carcinoma and evidence of common involvement of homocopolymer tracts in DNA microdeletions. Cancer Res. 1994; 54:3025–33. [PubMed: 8187092]
12. Maitra A, Adsay NV, Argani P, et al. Multicomponent analysis of the pancreatic adenocarcinoma progression model using a pancreatic intraepithelial neoplasia tissue microarray. Mod Pathol. 2003; 16:902–12. [PubMed: 13679454]
13. Hingorani SR, Petricoin EF, Maitra A, et al. Preinvasive and invasive ductal pancreatic cancer and its early detection in the mouse. Cancer Cell. 2003; 4:437–50. [PubMed: 14706336]
14. Jonkers J, Meuwissen R, van der Gulden H, et al. Synergistic tumor suppressor activity of BRCA2 and p53 in a conditional mouse model for breast cancer. Nat Genet. 2001; 29:418–25. [PubMed: 11694875]
15. Crook T, Brooks LA, Crossland S, et al. p53 mutation with frequent novel condons but not a mutator phenotype in BRCA1- and BRCA2-associated breast tumours. Oncogene. 1998; 17:1681–9. [PubMed: 9796697]
16. Skoulidis F, Cassidy LD, Pisupati V, et al. Germline Brca2 Heterozygosity Promotes Kras(G12D) -Driven Carcinogenesis in a Murine Model of Familial Pancreatic Cancer. Cancer Cell. 18:499–509. [PubMed: 21056012]
17. Bryant HE, Schultz N, Thomas HD, et al. Specific killing of BRCA2-deficient tumours with inhibitors of poly(ADP-ribose) polymerase. Nature. 2005; 434:913–7. [PubMed: 15829966]
18. Farmer H, McCabe N, Lord CJ, et al. Targeting the DNA repair defect in BRCA mutant cells as a therapeutic strategy. Nature. 2005; 434:917–21. [PubMed: 15829967]
19. Yuan SS, Lee SY, Chen G, et al. BRCA2 is required for ionizing radiation-induced assembly of Rad51 complex in vivo. Cancer Res. 1999; 59:3547–51. [PubMed: 10446958]
20. Daniels MJ, Wang Y, Lee M, et al. Abnormal cytokinesis in cells deficient in the breast cancer susceptibility protein BRCA2. Science. 2004; 306:876–9. [PubMed: 15375219]
21. Tutt A, Gabriel A, Bertwistle D, et al. Absence of Brca2 causes genome instability by chromosome breakage and loss associated with centrosome amplification. Curr Biol. 1999; 9:1107–10. [PubMed: 10531007]
22. Zhu L, Shi G, Schmidt CM, et al. Acinar cells contribute to the molecular heterogeneity of pancreatic intraepithelial neoplasia. Am J Pathol. 2007; 171:263–73. [PubMed: 17591971]
23. Thayer SP, di Magliano MP, Heiser PW, et al. Hedgehog is an early and late mediator of pancreatic cancer tumorigenesis. Nature. 2003; 425:851–6. [PubMed: 14520413]
24. Morris, JPt; Cano, DA.; Sekine, S., et al. Beta-catenin blocks Kras-dependent reprogramming of acini into pancreatic cancer precursor lesions in mice. J Clin Invest. 120:508–20. [PubMed: 20071774]
25. Rozenblum E, Schutte M, Goggins M, et al. Tumor-suppressive pathways in pancreatic carcinoma. Cancer Res. 1997; 57:1731–4. [PubMed: 9135016]
26. Goggins M, Hruban RH, Kern SE. BRCA2 is inactivated late in the development of pancreatic intraepithelial neoplasia: evidence and implications. Am J Pathol. 2000; 156:1767–71. [PubMed: 10793087]
27. Aguirre AJ, Bardeesy N, Sinha M, et al. Activated Kras and Ink4a/Arf deficiency cooperate to produce metastatic pancreatic ductal adenocarcinoma. Genes Dev. 2003; 17:3112–26. [PubMed: 14681207]
28. Bardeesy N, Cheng KH, Berger JH, et al. Smad4 is dispensable for normal pancreas development yet critical in progression and tumor biology of pancreas cancer. Genes Dev. 2006; 20:3130–46. [PubMed: 17114584]

29. Lewis BC, Klimstra DS, Varmus HE. The c-myc and PyMT oncogenes induce different tumor types in a somatic mouse model for pancreatic cancer. Genes Dev. 2003; 17:3127–38. [PubMed: 14681205]

30. Gidekel Friedlander SY, Chu GC, et al. Context-dependent transformation of adult pancreatic cells by oncogenic K-Ras. Cancer Cell. 2009; 16:379–89. [PubMed: 19878870]

31. Fong PC, Boss DS, Yap TA, et al. Inhibition of poly(ADP-ribose) polymerase in tumors from BRCA mutation carriers. N Engl J Med. 2009; 361:123–34. [PubMed: 19553641]

32. Tutt A, Robson M, Garber JE, et al. Oral poly(ADP-ribose) polymerase inhibitor olaparib in patients with BRCA1 or BRCA2 mutations and advanced breast cancer: a proof-of-concept trial. Lancet. 376:235–44. [PubMed: 20609467]

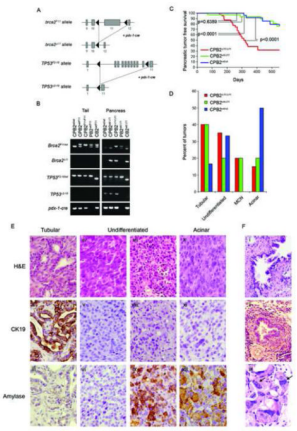

Figure 1. *Brca2* inactivation promotes pancreatic cancer when combined with *Trp53* inactivation

(A) Schematic representation of the *Brca2*^{F11} allele and the *Trp53*$^{F2\text{-}10}$ allele before and after pdx-1-cre dependent recombination. **(B)** PCR analysis demonstrating rearrangement of the *Brca2* and *Trp53* alleles in response to *pdx-1-cre* expression using DNA from mouse tail and pancreas. **(C)** Kaplan-Meier plots showing pancreatic cancer free survival of aged CPB2$^{\Delta 11/\Delta 11}$ (n=47), CPB2$^{wt/\Delta 11}$ (n=41), and CPB2$^{wt/wt}$ (n=34) mice. p- values were determined by a log rank test. **(D)** Frequency of histological subtypes of tumors detected in CPB2$^{\Delta 11/\Delta 11}$, CPB2$^{wt/\Delta 11}$ and CPB2$^{wt/wt}$ mice. **(E)** Representative images from tumors derived from CPB2$^{\Delta 11/\Delta 11}$ mice stained with H&E **(i,iv,vii,x),** cytokeratin 19 **(ii,v,viii,xi)** or amylase **(iii,vi,ix,xii). (F)** PanIN lesions (**i,ii**) and multinucleated cells (**iii**) from a CPB2$^{\Delta 11/\Delta 11}$ pancreas.

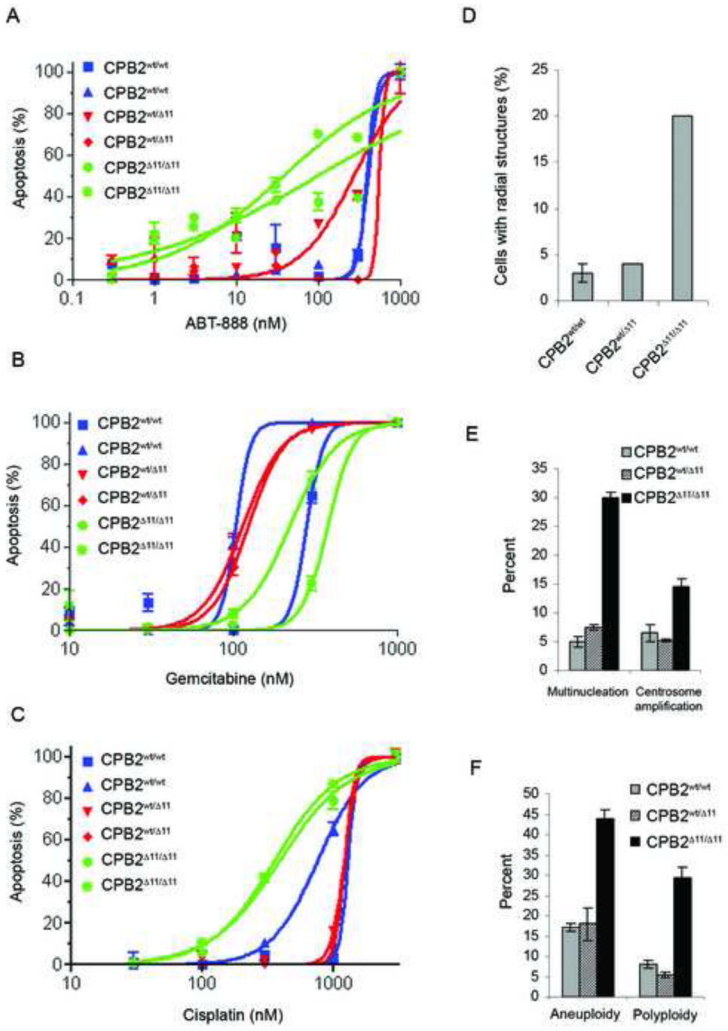

Figure 2. Inactivation of *Brca2* in pancreatic cancer cell lines induces sensitivity to DNA damage and promotes chromosomal instability

(A–C) Apoptosis in cell lines in response to ABT-888, gemcitabine, and cisplatin. **(D)** Quantification of radial structures in tumor cell lines treated with 100nM MMC. **(E)** Multinucleation and centrosome amplification in murine pancreatic tumor cell lines. **(F)** Aneuploidy and polyploidy in tumor cell lines with and without BRCA2.

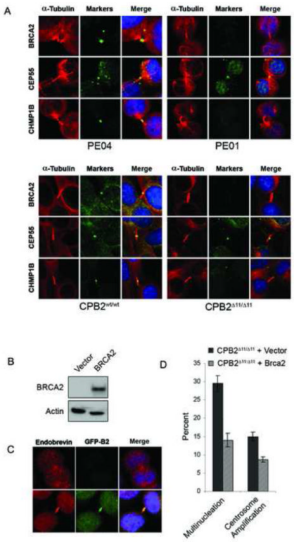

Figure 3. Inactivation of *Brca2* in pancreatic cancer cell lines disrupts localization of midbody proteins during cytokinesis

(A) Immunofluorescence images of intercellular bridges and midbody structures in tumor cell lines stained with antibodies against α-tubulin, BRCA2, CEP55, and CHMP1B. **(B)** Expression of BRCA2 in a reconstituted CPB2$^{\Delta 11/\Delta 11}$ cell line. **(C)** Immunofluorescence images showing the presence of endobrevin (red) and BRCA2 (green) at the midbody of a CPB2$^{\Delta 11/\Delta 11}$ cell line (top) reconstituted with GFP-BRCA2 (bottom). **(D)** Multinucleation and centrosome amplification measured by immunofluorescence in a CPB2$^{\Delta 11/\Delta 11}$ cell line reconstituted with empty vector or wild type BRCA2. Error bars represent SEM.

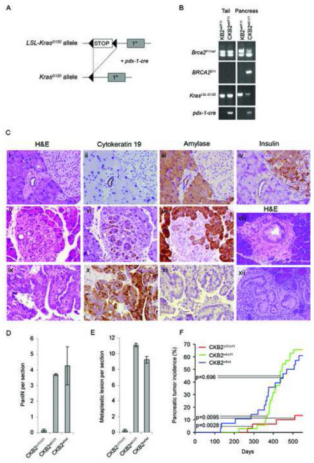

Figure 4. *Brca2* mutant alleles prevent development of premalignant lesions and pancreatic tumors in LSL-Kras^{G12D} mice

(A) Schematic representation of the *LSL-Kras^{G12D}* allele before and after *pdx-1-cre* dependent rearrangement. **(B)** PCR analysis of the *Brca2^{F11}* and *Kras^{G12D}* alleles in response to *pdx-1-cre* expression in the mouse tail and pancreas. **(C)** (i)H&E, (ii)cytokeratin 19, (iii)amylase and (iv)insulin staining of a normal pancreas from a CKB2$^{\Delta 11/\Delta 11}$ mouse. (v)H&E, (vi)cytokeratin 19 and (vii)amylase staining of a metaplastic lesion from a CKB2$^{wt/wt}$ mouse. (viii, xii)H&E staining of PanIN lesions from an 8-month old *Kras^{G12D}* mouse. (ix)H&E (x)cytokeratin 19 and (xi)amylase staining of a ductal tumor from a CKB2$^{\Delta 11/\Delta 11}$ mouse. **(D,E)** Quantitation of PanINs (D) and metaplastic lesions (E) from the pancreata of CKB2$^{wt/wt}$, CKB2$^{wt/\Delta 11}$ and CKB2$^{\Delta 11/\Delta 11}$ mice. Error bars represent SEM. **(F)** Tumor incidence in CKB2$^{\Delta 11/\Delta 11}$ mice (n=28), CKB2$^{wt/\Delta 11}$ mice (n=35) and CKB2$^{wt/wt}$ mice (n=30). p- values were determined by a log rank test.

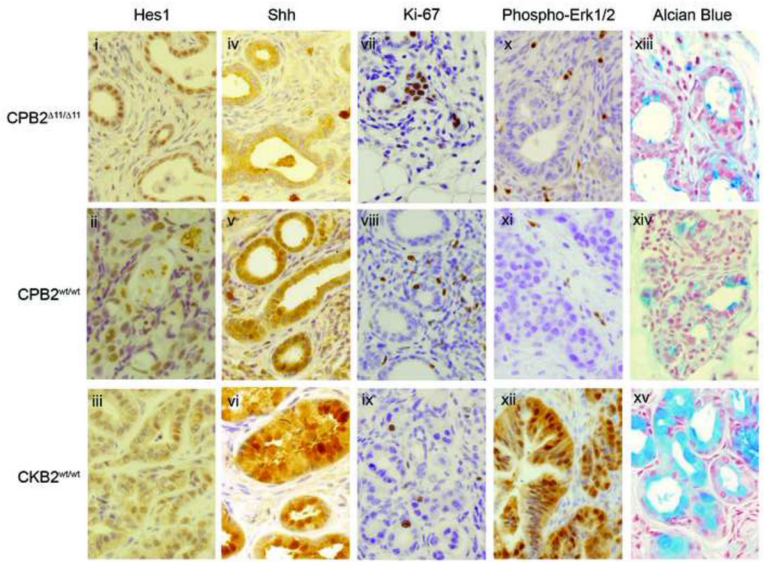

Figure 5. Tumors from CKB2$^{wt/wt}$, CPB2$^{wt/wt}$ and CPB2$^{\Delta 11/\Delta 11}$ mice display differences in biomarker expression

Representative images of pancreatic tumors from CPB2$^{\Delta 11/\Delta 11}$, CPB2$^{wt/wt}$, and CKB2$^{wt/wt}$ stained by IHC for (i–iii)Hes1, (iv–vi)Shh, (vii–ix)Ki-67, (x–xii)phospho-Erk1/2 and (xiii–xv)alcian blue dye.

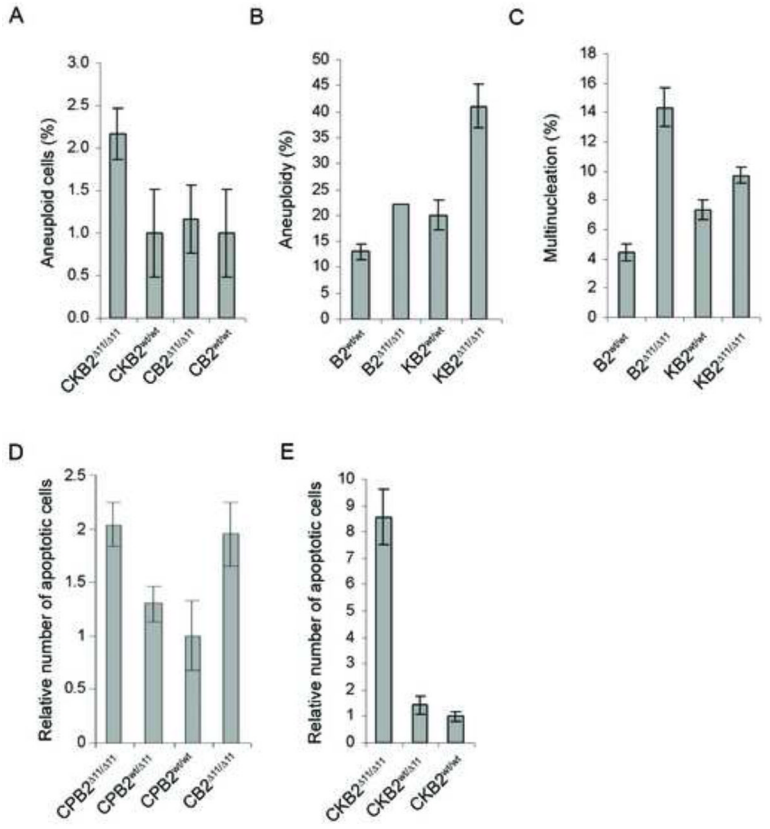

Figure 6. ***Brca2*** **mutant alleles promote chromosomal instability and apoptosis in mouse pancreatic tissue and MEFs**

(A) FISH analysis of pancreatic tissue from mice showing the percentage of cells with aneuploidy. **(B)** Metaphase spreads of MEFs scored for the presence of aneuploidy. **(C)** Percentage of MEFs with multinucleation measured by immunofluorescence microscopy after staining with α-tubulin antibody. **(D,E).** Quantitation of cleaved caspase 3 expression measured by IHC in the pancreas of 4 month old CPB2 and CB2 mice (D) and CKB2 (E) mice. Error bars represent SEM.

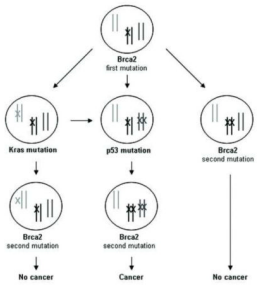

Figure 7. A model of *BRCA2* deficient tumorigenesis in the pancreas

The model reflects germline inheritance of a BRCA2 mutation. Inactivation of Tp53 signaling precedes inactivation or loss of the 2nd BRCA2 allele and facilitates cancer development. Early loss of the 2nd BRCA2 allele prior to disruption of Tp53 is inconsistent with cell growth/cell survival and tumor formation. Activation of Kras or other oncogenes prior to disruption of the 2nd BRCA2 allele is insufficient to maintain tumor formation if wildtype Tp53 signaling remains intact. Activation of oncogenes after inactivation of the 2nd BRCA2 allele and Tp53 signaling may promote tumor development.